Journal of Renewable Materials

Tech Science Press

DOI: 10.32604/jrm.2023.031503

ARTICLE

Bond-Slip Behavior of Steel Bar and Recycled Steel Fibre-Reinforced Concrete

Ismail Shah[1,2], Jing Li[1,3,4,*], Nauman Khan[5], Hamad R. Almujibah[6], Muhammad Mudassar Rehman[2], Ali Raza[7] and Yun Peng[3,4]

[1]School of Architecture and Civil Engineering, Yunnan Agricultural University, Kunming, 650000, China

[2]Institute of Mountain Hazards and Environment, Chinese Academy of Sciences, Chengdu, 610041, China

[3]Yunnan International Joint R&D Center of Smart Agriculture and Water Security, Yunnan Agricultural University, Kunming, 650201, China

[4]School of Water Conservancy, Yunnan Agricultural University, Kunming, 650201, China

[5]School of Civil Engineering, Guizhou University, Guiyang, 550025, China

[6]Department of Civil Engineering, College of Engineering, Taif University, P.O. Box 11099, Taif City, 21974, Saudi Arabia

[7]School of Civil Engineering, Zhengzhou University, Zhengzhou, 450001, China

[*]Corresponding Author: Jing Li. Email: li_jing69@163.com

Received: 22 June 2023 Accepted: 13 October 2023 Published: 23 January 2024

ABSTRACT

Recycled steel fiber reinforced concrete is an innovative construction material that offers exceptional mechanical properties and durability. It is considered a sustainable material due to its low carbon footprint and environmental friendly characteristics. This study examines the key influencing factors that affect the behavior of this material, such as the steel fiber volume ratio, recycled aggregate replacement rate, concrete strength grade, anchorage length, and stirrup constraint. The study investigates the bond failure morphology, bond-slip, and bond strength constitutive relationship of steel fiber recycled concrete. The results show that the addition of steel fibers at 0.5%, 1.0%, and 1.5% volume ratios can improve the ultimate bond strength of pull-out specimens by 9.05%, 6.94%, and 5.52%, respectively. The replacement rate of recycled aggregate has minimal effect on the typical bond strength of pull-out specimens. However, the ultimate bond strengths of pull-out specimens with concrete strength grades C45 and C60 have improved compared to those with C30 grade. The specimens with longer anchorage lengths exhibit lower ultimate bond strength, with a reduction of 33.19% and 46.37% for anchorage lengths of 5D and 7D, respectively, compared to those without stirrups. Stirrup restraint of 1 φ 8 and 2 φ 8 improves the ultimate bond strength by 5.29% and 6.90%, respectively. Steel fibers have a significant effect on the behavior of concrete after it cracks, especially during the stable expansion stage, crack instability expansion stage, and failure stage.

KEYWORDS

Recycled coarse aggregates (RCA); steel fiber; bonding performance; bond-slip; environmental challenges

1 Introduction

The construction industry, driven by the growing population demands, generates a substantial volume of waste, almost half comprising discarded concrete materials [1]. The outcome is the production of RCA, which involves partially or entirely substituting the obtained RA (Recycled Aggregates) with natural

aggregate NA in conventional concrete. RCA is a sustainable construction material that aims to reduce the utilization of NA while simultaneously converting waste materials into valuable resources. This innovative approach yields favorable economic viability, social well-being, and environmental sustainability outcomes. This process facilitates the recycling of a substantial quantity of generated garbage. Using a novel green construction material known as RCA is gaining increasing prominence in civil engineering owing to its numerous advantages [2]. Various researchers are currently engaged in developing ecological construction, which promotes the adoption of green, low-carbon, and circular growth in the building and construction sector [3–5]. The effective management and utilization of construction waste have become a critical challenge in the construction industry [6,7]. New urbanization, demolition, and renovation have generated significant construction waste. The conventional disposal of used concrete through stacking or landfilling pollutes the environment and consumes land resources. Alkaline substances in waste concrete increase soil alkalinity, reduce crop yield and threaten food security. Consequently, ecological and environmental challenges must be addressed in concrete production and disposal [8,9]. Recycled concrete offers considerable ecological and economic benefits compared to ordinary concrete [10,11].

The fundamental mechanical properties of RCA and the bonding performance between RCA and reinforcement play a crucial role in determining the feasibility of utilizing RCA in various practical engineering applications. Several researchers have been conducted on RCA's fundamental mechanical properties, as evidenced by the abundant scholarly material available. The findings derived from the research demonstrate that the RA's starting strength and substitution rate primarily influence RCA's mechanical properties [12,13]. Numerous scholars have directed their attention to examining the mechanical properties of recycled concrete, conducting both empirical and theoretical inquiries to explore its bonding qualities [14]. Prince et al. [15] investigated the bonding properties of recycled concrete, specifically examining the effects of deformed steel bars with 8 and 10 mm diameters in high-strength RCA. The concrete mixtures had replacement rates of recycled coarse aggregate at 25%, 50%, 75%, and 100% for both bar sizes. The study presents an empirical bond stress-slip relationship. It suggests that the anchorage lengths of deformed bars with two different diameters in high-strength recycled concrete can be considered equivalent to those in NA concrete of comparable strength.

Furthermore, the investigation observed that the normalized bond strength of recycled concrete improved as the percentage of RA replacement increased. Zhao et al. [16] investigated the energy interaction differences between corroded steel bars and recycled or NCA (Natural Coarse Aggregates). pull-out tests and beam tests were carried out. In stirrup specimens, the ultimate bond strength of RCA and NCA specimens did not differ with increasing reinforcement. Using stirrups minimized the variance in the bond characteristics of RCA and NCA specimens. Sindy et al. [17] experimented by replacing natural coarse aggregate with varying proportions of recycled coarse aggregate (20%, 50%, and 100%) and examined the bonding properties of RCA. The study concluded the bond strength difference depended on the RA replacement percentage. Hameed et al. [18] designed an experiment involving various concrete mixes with 0%, 50%, and 100% RAs, with and without fibres. Two kinds of fibres were examined separately: hooked-end steel and polypropylene fibres. The steel and polypropylene fibres used were 40 and 4.4 kg/m^3, respectively. Axial compression and standard pull-out tests were conducted on the specimens. The pull-out test specimens were made using deformed steel rebars of 19 mm (#6) diameter. The findings revealed that replacing NA with RA decreased the concrete's compressive strength. For the bond behavior of steel rebar, the research outcomes indicated that substituting 50% NA with RAs did not impact the bond response of the steel bar. However, replacing 100% of NA with RAs had an adverse effect on bond stress slip behavior.

Furthermore, He et al. [10] conducted a study that examined the effect of loading rate on the bond behavior of deformed steel bars in concrete. The research presented a bond stress-slip correlation for deformed steel bars, which considered loading rate, lateral pressure, concrete strength, and bar diameter

[19]. Rafi et al. [20] suggested a bond stress-slip constitutive law at the interface of steel bars in RCA. The existing model determines the ascending section of the bond stress-slip curve, and a modified expression is presented to reflect the descending area of the bond stress-slip curve. The bond-slip mechanism associated with the behavior of steel fibres taken out of concrete after high temperature was revealed by Fang et al. [21]. The outcomes demonstrated that heating significantly changed the binding behavior of straight fibres. With a steel fibre addition ratio of 0%, splitting failure is the primary failure mode of the central pull-out test specimens, and the bond-slip curves are incomplete. With a steel fibre addition ratio of 0.35% and 0.8%, splitting pull-out failure is the primary failure mode. With a steel fibre addition ratio of 1.5%, pull-out failure is the primary failure mode, and the integrity of the damaged specimens is good [19]. Kim et al. [22] studied the bond stress-slip behavior of 16 mm diameter deformed bars embedded in RCA with varying percentages of NA replaced with RA (0%, 30%, 60%, and 100%). The research revealed no significant difference in the bond behavior characteristics between NCA and RCA pull-out specimens during pre- and post-peak stages. Bilal et al. [23] conducted an experimental study to examine the effect of steel fibres on the bond strength of hooked bars in concrete with normal strength. The findings of the study revealed that incorporating steel fibres into the concrete mix led to a significant improvement in both peak load and ductility. Hameed et al. [24] conducted an experimental study to explore the bond stress-slip behavior of steel bars embedded in fibre-reinforced concrete. The researchers determined that incorporating fibres into the concrete mixture improved the bond stress-slip response across all loading stages, including pre-peak, peak, and post-peak loading.

Extensive research has been conducted on the bond strength between concrete that contains conventional aggregate and reinforcing steel bars. However, there is a limited number of studies that have investigated the bond qualities between RCA and steel bars. Several studies have indicated that the incorporation of RCA in concrete does not significantly impact the bond between steel reinforcing bars and reinforced RCA concrete. In fact, it has been observed that the bond strength may decrease by up to 10% when compared to conventional concrete [25]. One potential explanation for this phenomenon is that the strength of the bond is primarily influenced by the characteristics of the reinforcement, such as the surface profile and the type of steel rebar, rather than attributes associated with the aggregate materials [26]. However, it has been shown by some studies that the bond strength in concrete may exhibit an increase when the proportion of RCA is increased [27]. The enhanced bond strength observed in RCA can potentially be attributed to the heightened friction generated by the coarse texture of RCA particles. Another potential reason could be linked to the internal curing effect of RCA [26]. According to a study conducted by Kim et al. [28] it was shown that the increased replacement of RCA in concrete can potentially result in reduced bond strength between the deformed steel and the surrounding RCA concrete. This is attributed to the higher occurrence of air spaces in the concrete mixes [12].

This research investigates the bond-slip characteristics of steel bars in recycled steel fibre reinforced concrete incorporating steel fibres. Specifically, this study systematically examines the bond strength performance between steel bars and recycled steel fibre reinforced concrete, with five variables serving as controllable parameters: concrete strength grade, steel fibre volume ratio, recycled coarse aggregate replacement rate, anchorage length, and stirrup constraint.

2 Research and Methodology

2.1 Material

Conferring the Chinese national standard GB175-2007 [29], Ordinary Portland Cement (P.II 42.5) has a specific surface area of 356 m^2/kg and a compressive strength of 46.8 MPa at 28 days. This experiment utilized two types of coarse aggregate, natural coarse aggregate and recycled coarse aggregate. Both aggregates have a particle size range of 5 to 25 mm, and Table 1 shows the physical properties of NCA and RCA. River sand with a fineness modulus of 2.75 is used as fine aggregate.

Table 1: Physical property of coarse aggregate

Type	Apparent density kg/m^3	Bulk density kg/m^3	Crushing index %	Water absorption %	Porosity %	Mud content %	The total content of needle flakes %
Natural course aggregates	2370	1360	12.0	0.6	40	0.925	3.2
Recycled coarse aggregate	2660	1410	13.5	3.74	47	0.423	1.4

The end-hook steel fibre produced by Shanghai Bekaert Ergang Co., Ltd. (China) uses a fibre length-diameter ratio equal to lf/df = 35 mm / 0.55 mm = 64 and tensile strength of 1345 MPa. Jiangsu Sika Building Materials Co., Ltd. (China). High-performance superplasticizer/water reducer produces the water-reducing agent used in this experiment. While the longitudinal steel bar of the specimen was made of HRB400, and the horizontal stirrup was made of HPB335 steel bar [30]. Table 2 shows the steel bar's mechanical properties. Fig. 1 represents the physical typicals of coarse aggregates and steel fibres.

Table 2: Mechanical properties of steel bars

Type	Diameter ds/mm	Yield strength fy/MPa	Tensile strength fst/MPa	Elongation δst/%
HRB400	20	457	596	39.0
HRB335	8	325	493	41.3

(a) Natural coarse aggregates

(b) Recycled coarse aggregates

(c) Steel fibres

Figure 1: The physical characteristics of coarse aggregate and steel fibres

2.2 Test Parameters and Mix Design

The behaviors of bond-slip steel bars and high-strength recycled aggregate concrete with steel fibre were investigated using thirteen pull-out tests. The bonding performance of steel bar and steel fibre high-strength recycled concrete was studied systematically using five variables: concrete strength grade, recycled coarse aggregate replacement rate, steel fibre volume rate, anchorage length, and stirrup constraint. For example, C45R100F1-100-2 represented the concrete strength grade of specimen C45, the replacement concentration of recycled coarse aggregate was 100%, the volume content of steel fibres was 1.0%, anchorage length (60, 100, 140 mm), and Stirrup Constraints comparing different levels of stirrup

constraint: no stirrups (0), one row of 8 stirrups (1 φ 8), and two rows of 8 stirrups (2 φ 8). Table 3 displays the test specimen design parameters, and Fig. 2 shows the precise measurements and components of the test specimens.

Table 3: Specimen design parameters

Groups	Concrete strength grade	Replacement rate of RA r_g/%	Steel fibre volume ratio v_f/%	Anchor length l_a/mm	Stirrup constraints
C45R0F0-100-2	C45	0	0	100	2 Rows of 8 stirrups
C45R100F1-100-2	C45	100%	1.00%	100	2 Rows of 8 stirrups
C45R100F0-100-2	C45	100%	0.00%	100	2 Rows of 8 stirrups
C45R100F05-100-2	C45	100%	0.50%	100	2 Rows of 8 stirrups
C45R100F15-100-2	C45	100%	1.50%	100	2 Rows of 8 stirrups
C45R0F1-100-2	C45	0%	1.00%	100	2 Rows of 8 stirrups
C45R50F1-100-2	C45	50%	1.00%	100	2 Rows of 8 stirrups
C30R100F1-100-2	C30	100%	1.00%	100	2 Rows of 8 stirrups
C60R100F1-100-2	C60	100%	1.00%	100	2 Rows of 8 stirrups
C45R100F1-60-2	C45	100%	1.00%	60	2 Rows of 8 stirrups
C45R100F1-140-2	C45	100%	1.00%	140	2 Rows of 8 stirrups
C45R100F1-100-0	C45	100%	1.00%	100	0
C45R100F1-100-1	C45	100%	1.00%	100	1 Row of 8 stirrups

The Concrete Mix Proportion Design Regulations “GJG55-2011” national standards for China are used in this work. The mix ratio of steel fibre high-strength recycled concrete is initially determined. The standard cube compressive strength test of concrete is carried out, and the mix ratio for high-strength steel fibre recycled concrete that meets the test requirements is obtained. Table 4 displays the mix ratio of high-strength recycled concrete and steel fibre used. The specimen C45R0F0-100-2 contains 0% RCA as well as steel fibres, giving a compressive strength of 52.7 MPa.

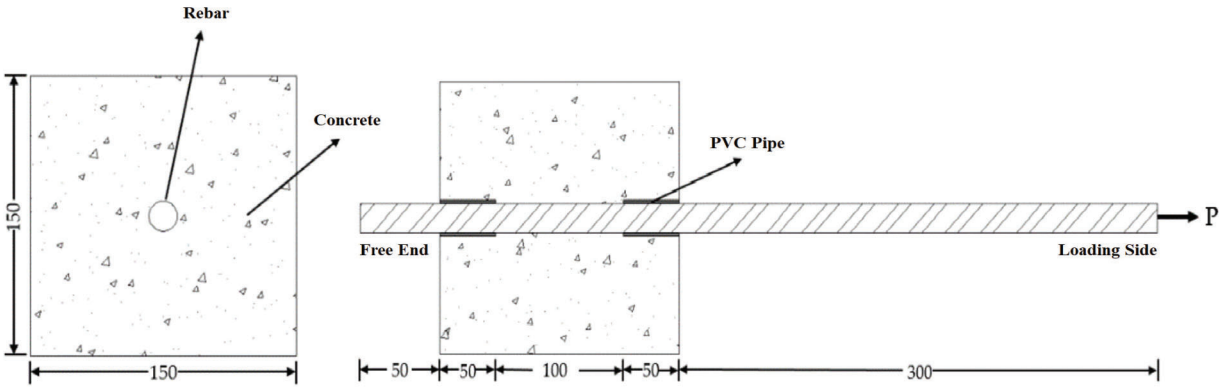

(a) Designed size.

(b) Physical object of the test specimen.

Figure 2: Specimen design size and physical shape

Table 4: Mix design of high-strength recycled concrete and steel fibre

Group	Material consumption/(kg·m^{-3})							
	Water	Cement	NCA	RCA	Sand	Steel fibre	Water reducer	Additional water
C45R0F0-100-2	180	471	997	0	752	0	0.94	0
C45R100F1-100-2	180	471	0	997	752	78	0.94	23.52
C45R100F0-100-2	180	471	0	997	752	0	0.94	23.52
C45R100F05-100-2	180	471	0	997	752	39	0.94	23.52
C45R100F15-100-2	180	471	0	997	752	117	0.94	23.52
C45R0F1-100-2	180	471	997	0	752	78	0.94	0
C45R50F1-100-2	180	471	498	498	752	78	0.94	11.76
C30R100F1-100-2	180	332	0	1038	850	78	0.66	24.50
C60R100F1-100-2	200	663	0	891	645	78	1.33	21.04
C45R100F1-60-2	180	471	0	997	752	78	0.94	23.52
C45R100F1-140-2	180	471	0	997	752	78	0.94	23.52
C45R100F1-100-0	180	471	0	997	752	78	0.94	23.52
C45R100F1-100-1	180	471	0	997	752	78	0.94	

2.2.1 Measurement Method

After checking that the appearance and dimensions of the specimen are intact, proceed to position it at the central location of the universal testing machine. Secure the loading end tightly using the appropriate fixture. Subsequently, attach five displacement gauges to the specimen's bottom surface, free end, and loading end, respectively. Establish a connection with the displacement acquisition device and ensure the equilibrium of the displacement acquisition system. Begin by applying a preload of 3 kN, then initiate the universal testing machine and dynamic data acquisition system (DH5922D). Employ displacement control to apply the load. Monitor the slip value of the free end of the steel bar until it reaches the spacing between the transverse ribs. Once the concrete undergoes splitting and failure, the testing process concludes. At this point, the specimen is extracted, and the failure morphology of the specimen is examined. In order to ascertain the relative slip occurring at the loading end of the reinforced steel fiber high-strength recycled concrete specimen, a method was employed involving the placement of two displacement gauges on a fixture supported by the steel bar. The resulting measurements were averaged to obtain the loading end slip. A displacement gauge is utilized to measure the displacement of the steel bar's free end by measuring the specimen's free end, to mitigate the impact of concrete compression deformation on the slip of the free end, displacement gauges are installed on either side of the steel bar to quantify the compression deformation of the concrete. The configuration of the displacement gauge is depicted in Fig. 3.

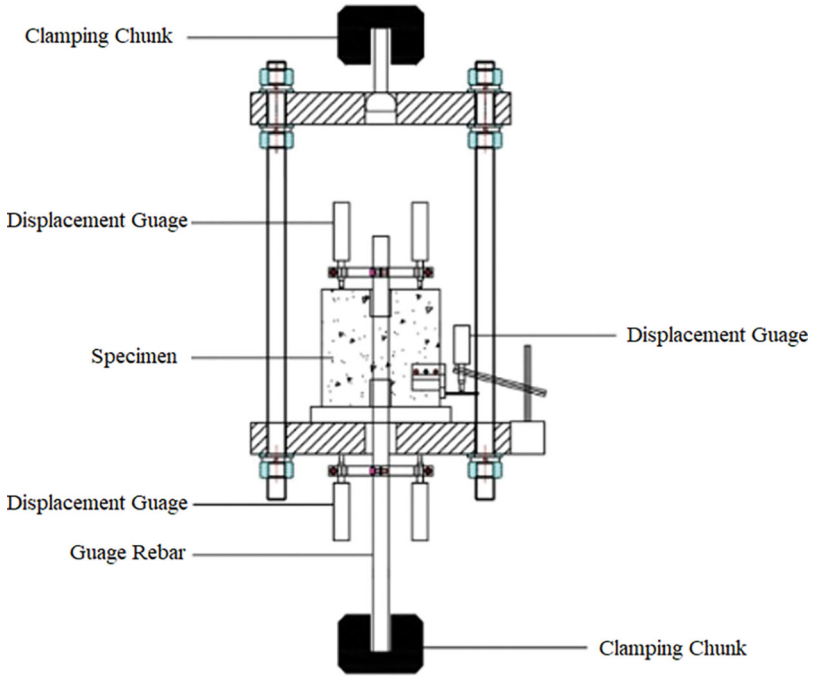

Figure 3: The configuration of the displacement gauge

2.2.2 Specimen Fabrication and Concrete Compression Test

The test molds of the reinforced steel fibre high-strength recycled concrete specimens are made of wooden formwork with a thickness of 10 mm, and holes are drilled on both sides of the wooden formwork for the steel bars to pass through. The processed wooden formwork is placed flat on the pouring site. Reinforcing bars and transverse stirrups are placed within the formwork. Before pouring the test specimens, the PVC pipe was placed over the unbonded area of the concrete and steel bar. In the

pouring of pull-out specimens, each group was poured with three 150 mm × 150 mm × 150 mm standard cube test blocks. After curing for 28 days, the cube test blocks were subjected to a compression test. Fig. 4 shows the test specimens of compression test results.

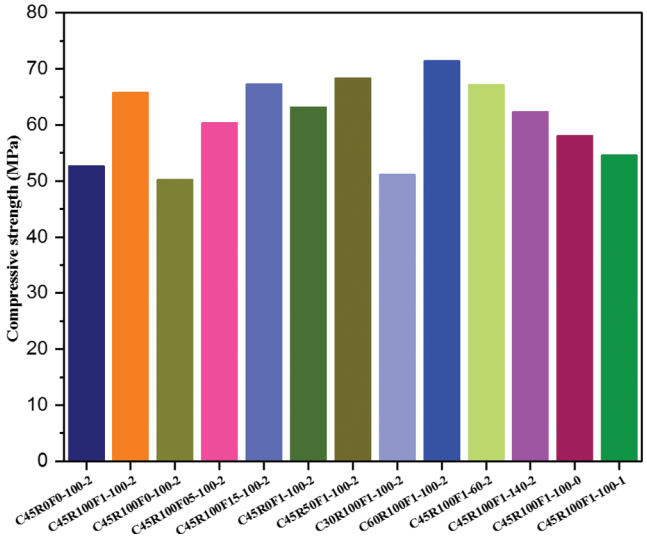

Figure 4: Compressive strength of recycled steel fibre reinforced concrete specimens

2.2.3 Test Loading Procedure

The reinforced steel fibre high-strength recycled concrete specimen was tensile tested with a maximum test force of 1000 kN using a universal testing machine. A particular reaction frame is designed to achieve the actual loading boundary conditions, connected by two fast-thick steel plates and four threaded steel bars. Displacement control is used to apply the load at 0.30 mm/min. Measure the displacement at each location with a displacement meter. An acquisition system for dynamic strain data was used to connect all instruments. When the slip value of the free end exceeds 25 mm, the loading process is terminated.

3 Results

To calculate the ultimate bond strength, τu, we assume that the bond stress is uniformly distributed along the anchorage length, la. The bond strength can thus be calculated using Eq. (1). Eq. (1) allows us to isolate and quantify the specific contribution of each parameter to the ultimate bond strength, thereby enabling a more precise understanding of the behavior under study.

$$\tau_u = \frac{P_{max}}{\pi \times \mathrm{ds} \times \mathrm{la}} \tag{1}$$

where,

τ_u is the ultimate bond strength.

P_{max} the maximum pull-out load

ds is the diameter of the steel bar's

la is the length anchorage.

The bond-slip curve's comprehensive strength was evaluated for the measured steel bar and the recycled steel fibre-reinforced concrete bond samples. Loaded-end eigenvalues are presented in Table 5, while measured free-end eigenvalues are shown in Table 6. As observed, the bond-slip curve's eigenvalues are

subject to multiple factors, such as the concrete's strength, the volume fraction of steel fibres, stirrup restraint, replacement ratio for recycled materials, and the length of the anchorage.

Table 5: Typical values of loading end

Group	Yield slip Ss/kN	Crack bond strength τ_s/MPa	Limit slip Su/kN	Ultimate bond strength τ_u/MPa	Residual slip Sr/kN	Residual bond strength τ_r/MPa
C45R0F0-100-2	0.84	15.46	6.01	28.55	14.38	11.61
C45R100F1-100-2	1.22	20.62	10.42	27.88	15.26	22.09
C45R100F0-100-2	2.46	14.39	7.67	26.07	16.07	14.30
C45R100F05-100-2	0.87	19.91	7.47	28.43	14.14	20.17
C45R100F15-100-2	1.39	21.61	14.56	27.51	24.46	24.65
C45R0F1-100-2	1.38	20.74	15.73	27.66	22.49	23.07
C45R50F1-100-2	0.97	20.77	18.17	28.96	26.83	22.47
C30R100F1-100-2	1.67	22.02	6.49	25.75	14.12	18.33
C60R100F1-100-2	1.60	21.26	9.66	27.95	11.44	21.87
C45R100F1-60-2	0.99	37.01	6.65	41.73	23.31	36.94
C45R100F1-140-2	1.13	16.14	21.50	22.38	26.68	16.04
C45R100F1-100-0	1.13	21.39	7.13	26.08	28.86	14.18
C45R100F1-100-1	0.91	21.76	8.39	27.46	26.18	18.25

Table 6: Values of the free end

Group	Yield slip Su/kN	Ultimate Bond Strength τ_u/MPa	Residual slip Sr/kN	Residual Bond Strength τ_r/MPa
C45R0F0-100-2	0.005	28.55	8.85	14.30
C45R100F1-100-2	0.28	27.88	6.42	22.09
C45R100F0-100-2	0	26.07	7.61	11.61
C45R100F05-100-2	0.61	28.90	6.31	18.60
C45R100F15-100-2	1.48	27.51	10.95	24.65
C45R0F1-100-2	0.19	27.66	6.80	23.07
C45R50F1-100-2	0.09	28.96	6.79	22.47
C30R100F1-100-2	0.18	25.59	6.37	18.20
C60R100F1-100-2	0.55	28.70	6.19	21.77
C45R100F1-60-2	0.95	41.74	16.62	36.94
C45R100F1-140-2	0.11	22.76	5.66	14.14
C45R100F1-100-0	0	26.40	13.45	10.97
C45R100F1-100-1	0.07	26.16	18.23	18.25

The tables, specifically Tables 5 and 6, depict the comparative advantage of recycled steel fibre-reinforced concrete and steel bars to their ultimate bond strength. The bond strength values observed range from 22.38 to 28.96 MPa. Further analysis was conducted to determine the individual influence of each factor on the crack bond strength τ_s, residual bond strength τ_r, and ultimate bond strength τ_u. Based on the testing results of the 13 groups of recycled steel fibre-reinforced concrete bond pull-out specimens, a statistically-regressed formula was derived for calculating the typical bond strength.

1. Crack bond strength at the loading end

$$\tau_s = f_{cu} \cdot \left(0.72127 - 1.24637v_f - 0.0673r_g + 0.11411{r_g}^2 - 0.07484 \cdot \frac{l_a}{d} - 3.85569\rho_s\right)$$

2. Ultimate bond strength at the loading end

$$\tau_u = f_{cu} \cdot \left(0.86096 - 3.45846v_f - 0.15002r_g + 0.12894{r_g}^2 - 0.06724 \cdot \frac{l_a}{d} - 3.58596\rho_s\right)$$

3. Residual bond strength at the loading end

$$\tau_r = f_{cu} \cdot \left(0.52391 + 9.95086v_f - 0.08002r_g + 0.08813{r_g}^2 - 0.07497 \cdot \frac{l_a}{d} + 14.61274\rho_s\right)$$

where, v_f is the volume fraction of steel fibres, r_g is the replacement concentration of RAs, l_a is the anchorage length, l_a is a fixed length of steel bar, d is the steel bar diameter, and f_{cu} is the compressive strength of the recycled steel fibre reinforced concrete specimens.

Two mathematical equations have been utilized to calculate the free end's residual and ultimate bonding strength.

4. Ultimate bond strength of a free end

$$\tau_u = f_{cu} \cdot \left(0.84799 - 3.56741v_f - 0.15062r_g + 0.13194{r_g}^2 - 0.06579 \cdot \frac{l_a}{d} - 2.63086\rho_s\right)$$

5. Residual bond strength at a free end

$$\tau_r = f_{cu} \cdot \left(0.51944 + 10.34663v_f - 0.07912r_g + 0.07983{r_g}^2 - 0.08223 \cdot \frac{l_a}{d} + 20.35003\rho_s\right)$$

After comparing the experimental and regression calculation values, as shown in Tables 7 and 8, it becomes apparent that the regression formula effectively represents the bond strength relationship of the components under investigation. The results mentioned above offer significant theoretical backing for the practical use of engineering technology, highlighting the significance of regression analysis in effectively forecasting bond strength.

Table 7: Comparison of the bond strength properties based on test results and loading end

Group	Crack bond strength			Ultimate bond strength			Residual bond strength		
	Test value	Calculated	Ratio	Test value	Calculated	Ratio	Test value	Calculated	Ratio
C45R0F0-100-2	15.46	16.93	0.91	28.55	26.39	1.08	11.61	13.02	0.89
C45R100F1-100-2	20.62	23.40	0.88	27.88	29.29	0.95	22.09	23.33	0.95
C45R100F0-100-2	14.39	14.19	1.01	26.07	28.92	0.90	14.3	15.38	0.93
C45R100F05-100-2	19.91	21.85	0.91	28.43	27.93	1.02	20.17	18.41	1.10
C45R100F15-100-2	21.61	23.51	0.92	27.51	28.79	0.96	24.65	27.21	0.91
C45R0F1-100-2	20.74	19.51	1.06	27.66	29.46	0.94	23.07	21.90	1.05
C45R50F1-100-2	20.77	20.77	1.00	28.96	28.96	1.00	22.47	22.47	1.00
C30R100F1-100-2	22.02	18.21	1.21	25.75	22.79	1.13	18.33	18.16	1.01
C60R100F1-100-2	21.26	25.39	0.84	27.95	31.78	0.88	21.87	25.32	0.86
C45R100F1-60-2	37.01	33.95	1.09	41.73	38.95	1.07	36.94	33.90	1.09
C45R100F1-140-2	16.14	12.85	1.26	22.38	19.38	1.15	16.04	12.77	1.26
C45R100F1-100-0	21.39	22.16	0.97	26.08	27.26	0.96	14.18	14.91	0.95
C45R100F1-100-1	21.76	20.12	1.08	27.46	24.96	1.10	18.25	16.69	1.09
Error analysis	Average: 1.01393			Average: 1.01078			Average: 1.00665		
	Standard deviation: 0.01479			Standard deviation: 0.00736			Standard deviation: 0.01101		

Table 8: Comparison of calculation results of specimen bond strength of a free end

Group	Ultimate bond strength			Residual bond strength		
	Test values	Calculated	Ratio	Test values	Calculated	Ratio
C45R0F0-100-2	28.55	26.42	1.08	11.61	12.89	0.90
C45R100F1-100-2	27.88	29.42	0.95	22.09	22.95	0.96
C45R100F0-100-2	26.07	29.11	0.90	14.3	14.80	0.97
C45R100F05-100-2	28.90	28.08	1.03	18.6	17.94	1.04
C45R100F15-100-2	27.51	28.89	0.95	24.65	26.96	0.91
C45R0F1-100-2	27.66	29.43	0.94	23.07	22.00	1.05
C45R50F1-100-2	28.96	28.96	1.00	22.47	22.47	1.00
C30R100F1-100-2	25.59	22.89	1.12	18.20	17.86	1.02
C60R100F1-100-2	28.70	31.92	0.90	21.77	24.91	0.87
C45R100F1-60-2	41.74	38.88	1.07	36.94	34.49	1.07
C45R100F1-140-2	22.76	19.68	1.16	14.14	11.50	1.23
C45R100F1-100-0	26.40	27.00	0.98	10.97	12.35	0.89
C45R100F1-100-1	26.16	24.89	1.05	18.25	15.32	1.19
Error analysis	Average: 1.00932			Average: 1.00783		
	Standard deviation: 0.00636			Standard deviation: 0.01117		

3.1 Steel Fibre Volume Ratio

Fig. 5 illustrates the bond-slip curves for pull-out specimens exhibiting different steel fibre volume percentages, namely 0%, 0.5%, 1.0%, and 1.5%. The slip displacement of steel bars exhibits a positive correlation with the increase in steel fibre content [19,31]. However, the bond strength gradually improves and subsequently decreases. When the steel fibre content is 0%, the cracks rapidly expand due to the lack of restraint once the bond strength reaches its maximum, resulting in a swift drop in bonding strength until it disappears.

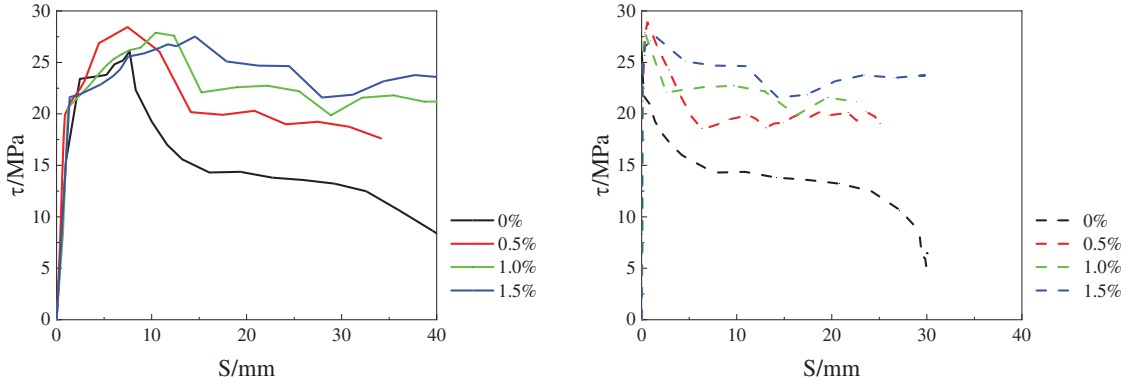

(a) Bond slip curve at loading end (b) Bond slip curve at a free end

Figure 5: Steel fibre volume ratio's influences on the bond-slip curve

As the volume fraction of steel fibres increases, the bond strengths of the bond-slip curve's ascending, descending, and smooth ends tend to rise in the pull-out specimens. The addition of steel fibres hinders the formation of cracks in the specimen [32], significantly lowering the bond-slip curve in pull-out specimens with a steel fibre content of 1.5%. Furthermore, the delaying effect is more pronounced with higher concentrations of steel fibres.

Fig. 6 shows the relationship between the steel fibers' volume proportion and the bond strength behavior on the bond-slip curve. The study's findings indicate that the incorporation of steel fibres positively impacts both crack bond strength and recycling bond strength, with an increase in fibre content. However, it is seen that the final bond strength tends to decrease as the fibre content is further increased. An obstruction that prevents proper contact between the mortar and aggregate during the process of concrete mixing results in the forming of a weakened layer within the concrete, ultimately hampering the improvement of bond strength. The ultimate bond strength of the pull-out specimens exhibited an increase of 9.05%, 6.94%, and 5.52% at steel fibre volume ratios of 0.5%, 1.0%, and 1.5%, respectively, compared to the specimens without any steel fibre additions.

3.2 Replacement Proportion/Content of RA

The bond-slip curves of pull-out specimens with different proportions of recycled aggregate (RA) replacement, specifically 0%, 50%, and 100%, are illustrated in Fig. 7. The increasing slope of the bond-slip curve indicates that the pull-out specimens containing 100% recycled aggregate (RA) tend to reach their maximum bond strength at the loaded end while displaying negligible slip along the ascending slope of the free end. There is a notable disparity in the lowering slope of the bond-slip curve among the three groups of pull-out specimens. Specifically, as the replacement content of recycled material increases, the slope exhibits a more pronounced decrease.

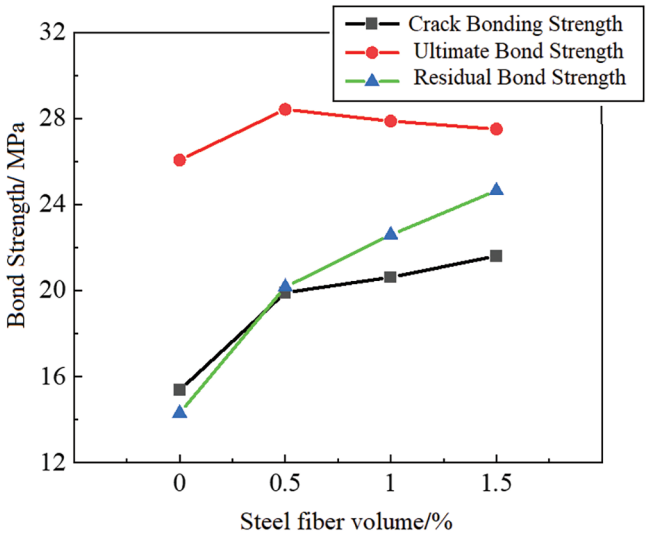

Figure 6: Steel fibre volume ratio's impact on the typical bond strength

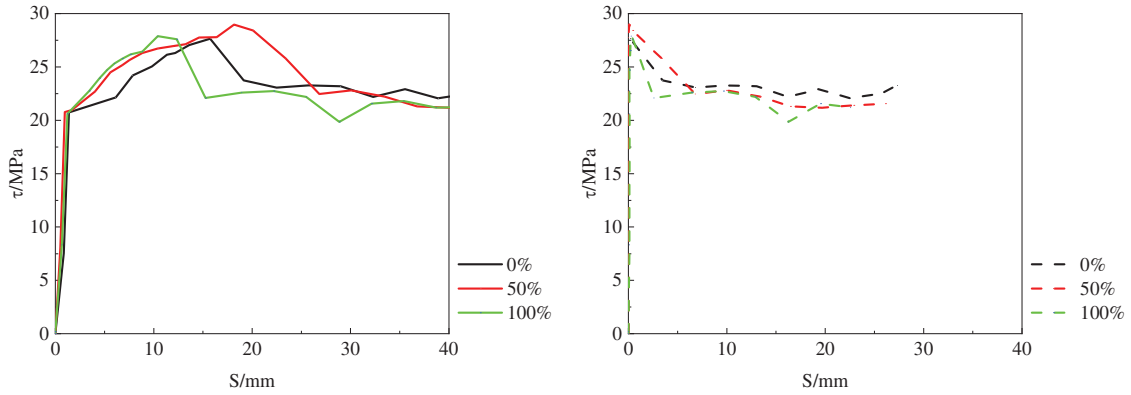

Figure 7: Effects of replacement content for RAs on the bond slip curve

Fig. 8 illustrates the influence of replacing RA content on the characteristic bond strength of the bond-slip curve. The findings indicate that the substitution rate of RA has a negligible effect on the overall bond strength, recycling bond strength, and cracking bond strength. Nevertheless, the substitution of content has a discernible impact on the slip related to the residual bond strength and the ultimate bond strength, as illustrated by the bond-slip curve.

3.3 Concrete Strength Grades

The bond-slip curves of pull-out specimens for concrete grades C30, C45, and C60 are presented in Fig. 9. The experimental results indicate that the bond-slip curve of the test specimen exhibits an upward trend as the concrete grade increases. Furthermore, the rate of decline in the descending region of the curve also shows an increasing trend. This observation indicates that the inhibitory impact of steel fiber on concrete diminishes as the concrete grade ascends while maintaining a constant volume ratio of steel fiber. Furthermore, the bonding strength of the pull-out specimens generally improves as the concrete

strength grade increases. The observed phenomenon can be ascribed to increased concrete density at higher grades, enhancing chemical adhesion force, mechanical occlusal force, and splitting tensile strength. This helps prevent the development of internal fractures in the pulled-out specimen and increases stickiness.

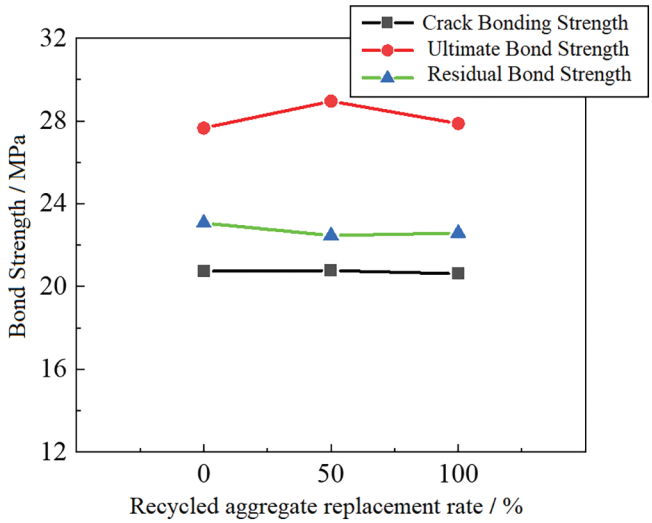

Figure 8: Impact of replacement concentration of RA on typical bond strength

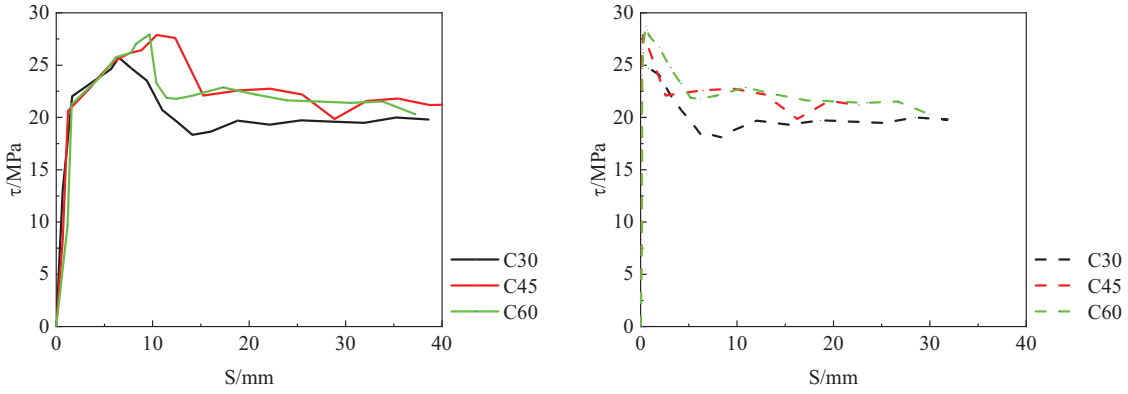

(a) Bond slip curve at loading end (b) Bond slip curve at a free end

Figure 9: Grade of concrete's strength and its impact on the bond-slip curves

Fig. 10 displays the impact of concrete strength grade on the typical bond strengths and bond-slip curve. The results indicate that the ultimate and recycled bond strength tend to improve as the concrete strength grade increases. For instance, the ultimate bond strength of specimens with C45 and C60 grades increased by 8.27% and 8.54%, respectively, compared to tensile specimens with grade C30. These findings suggest that the strength of the concrete plays a crucial role in the bonding behavior of the specimens, with higher grades of concrete exhibiting enhanced bonding characteristics. This highlights the importance of considering the grade of concrete strength in designing and constructing structures that require strong bonding performance.

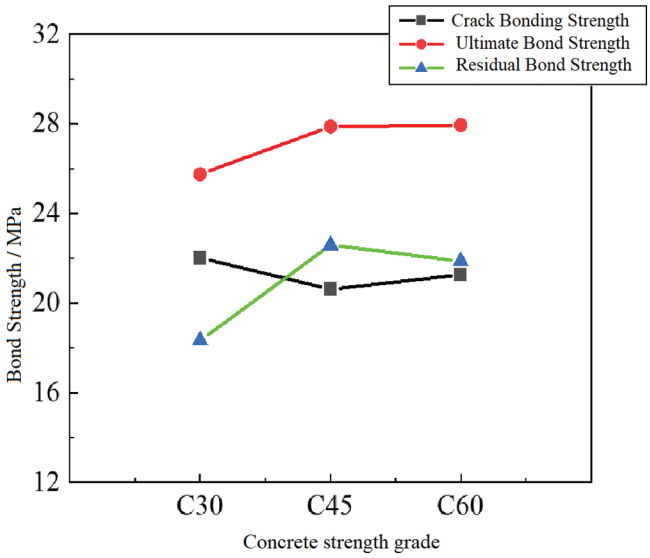

Figure 10: Impact of concrete strength grade on bond strength

3.4 Anchorage Length

Fig. 11 depicts the bond-slip curves of pull-out specimens for three different 3D, 5D, and 7D anchor lengths. The results indicate that as the anchorage length increases, the slope on the bond-slip curve gradually becomes gentler, with a sequential decrease in bond strength. In non-linear distribution, longer bond sections result in more uneven bonding stress distribution on the steel bar surface after the specimen is stressed, reducing bonding strength against damage. These findings underscore the importance of considering the anchorage length in determining the bonding behavior of pull-out specimens. Thus, the anchorage length should be optimized for concrete structures to achieve maximum bonding strength and prevent damage.

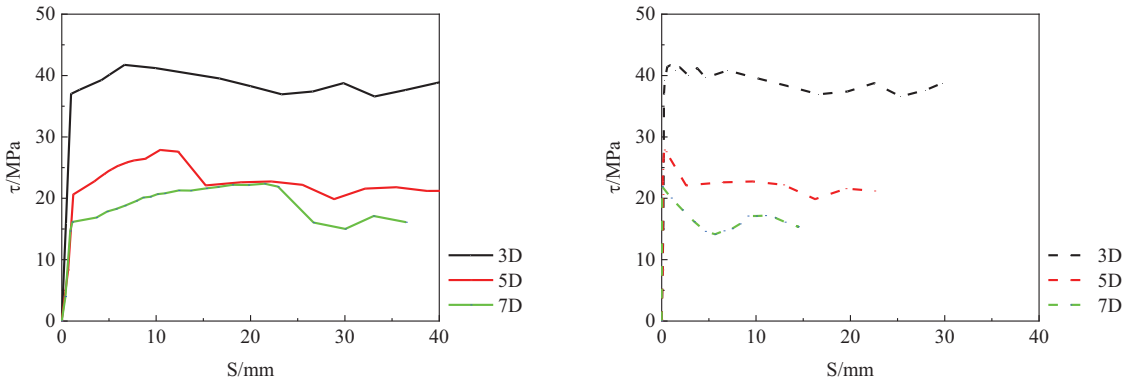

(a) Bond slip curve at loading end (b) Bond slip curve at a free end

Figure 11: Anchorage length effects on the bond-slip curve

Fig. 12 presents the impact of anchoring length on bond strength typicals. The results indicate that the ultimate bond strength, fracture bond strength, and residual bond strength decrease as the anchoring length increases. For instance, compared to pull-out specimens with 3D anchorage lengths, the ultimate bond

strength of pull-out specimens with 5D and 7D anchorage lengths decreased by 33.19% and 46.37%, respectively. These findings highlight the importance of considering the anchoring size in designing concrete structures to prevent damage and achieve optimal bonding strength.

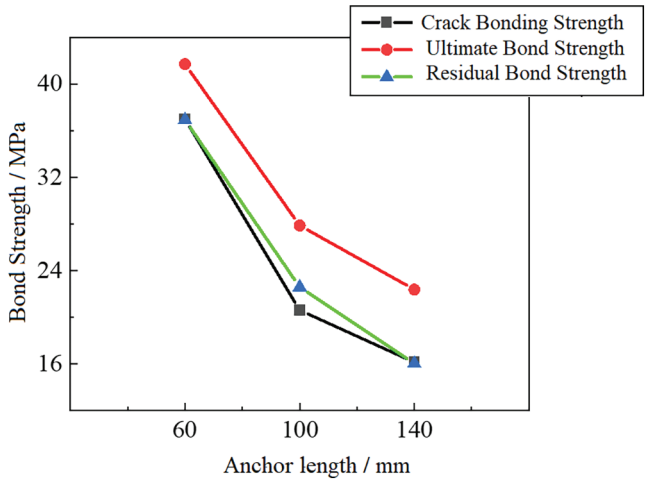

Figure 12: Influences of anchoring length on bond strength properties

3.5 Stirrup Constraints

Fig. 13 shows the bond-slip curves on pull-out specimens for stirrup constraints of 0, 1 φ 8 and 2 φ 8, respectively. The figure indicates the stirrup restraint's bond-slip curve and the pull-out specimen has a much stronger bond than the pull-out specimen without the stirrup restraint. When there are stirrups, the stirrups and the concrete will jointly cause the tensile force generated by the bonding force so that the hoop tensile stress on the concrete is reduced, the splitting cracks inside the specimen is suppressed, and the adhesion is decreased between steel bar and concrete. There has been no significant improvement in the steel bar and concrete and its bonding strength, from 1 φ 8 to 2 φ 8, because the confinement range of the stirrups inside the specimen was limited, and the development of cracks could not be suppressed entirely.

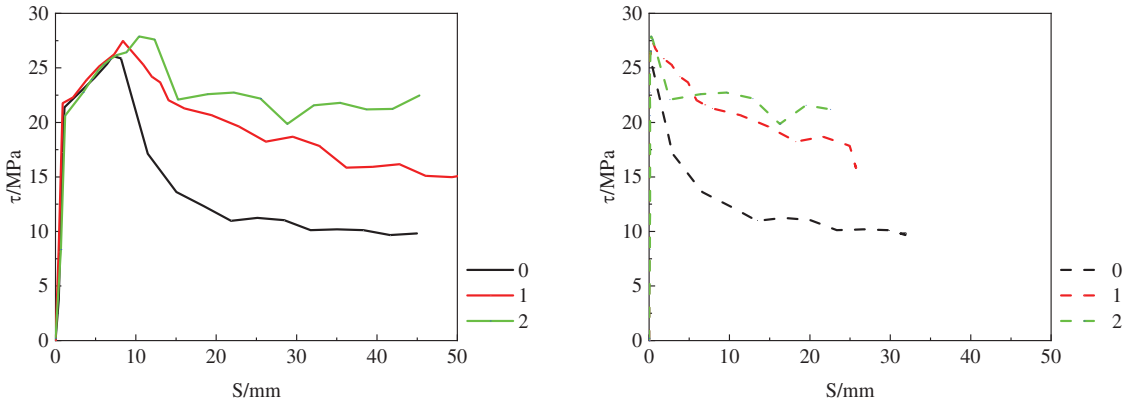

(a) Bond slip curve at the loading end (b) Bond slip curve at the free end

Figure 13: Stirrup restraint impacts the bond-slip curve

Fig. 14 shows the impacts of stirrup restraint on the typical bond strength on a bond-slip curve. It can be seen from the figure that the ultimate bond strength tends to increase with the increase of stirrup restraint. Compared with the pull-out specimens unrestrained by stirrups., the ultimate bond strength of the pull-out specimens with stirrup restraint of 1 φ 8 and 2 φ 8 increased by 5.29% and 6.90%, respectively.

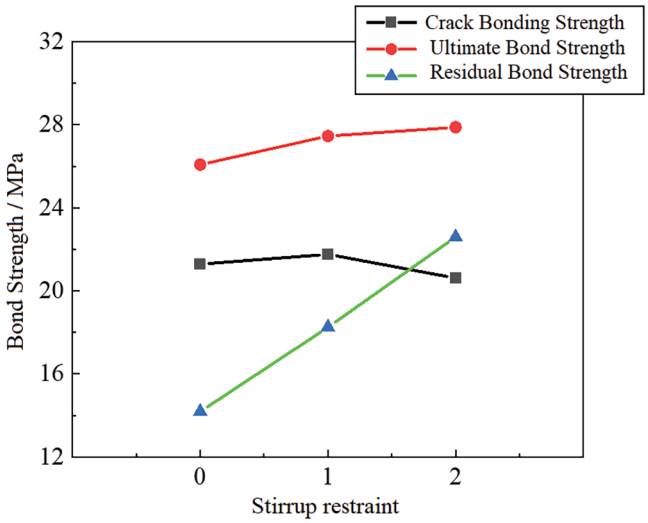

Figure 14: Stirrup restraint's impacts on the bond strength

4 Conclusion

This work investigates the bond failure characteristics of reinforced concrete incorporating steel bars and recycled steel fibre. Specifically, the focus is on analyzing the bond-slip and bond strength relationship under monotonic loading conditions. Thirteen center pull-out specimens were constructed using steel and recycled fiber-reinforced concrete. The experimental findings indicated the occurrence of two distinct mechanisms of failure: reinforcement pull-out failure and splitting failure. A mathematical equation was formulated to represent the bond strength between steel and recycled steel fiber-reinforced concrete, considering multiple elements that impact the bond-slip behavior. The impact of the RA replacement rate on the bond strength, as assessed using pull-out specimens, is minimal.

In contrast to specimens with a C30 grade, the bond strengths of pull-out specimens with concrete strength grades C45 and C60 have exhibited an augmentation. When comparing specimens with longer anchoring lengths to those without stirrups, it is observed that the specimens with longer anchorage lengths show a reduced ultimate bond strength. Specifically, there is a decrease of 33.19% and 46.37% in maximum bond strength for anchorage lengths of 5D and 7D, respectively. The use of stirrup constraint at ratios of 1 φ 8 and 2 φ 8 results in respective improvements of 5.29% and 6.90% in the final bond strength. The insertion of steel fibres can considerably modify the behavior of cracked concrete, notably during the stable expansion stage, crack instability expansion stage and collapse stage of the material. The bonding and friction force combination primarily determines the adhesive strength between steel bars and fiber-reinforced concrete. The mechanical interlocking force between the reinforcement and the concrete predominantly drives this bonding strength. Steel fibres in concrete offer mechanical anchoring, which mitigate bond-slip and provide crack-limiting and crack-resistant properties to the material. The bond-slip behavior can be categorized into distinct stages based on stress levels.

The load-slip curve of the test specimen is examined and condensed. The load-slip curve of the test specimen can be categorized into five distinct stages of slip: micro-slip stage, internal fracture slip stage, pull-out stage, drop stage, and residual stage. Additional investigation is required to thoroughly examine the failure process and the shape of cracks, employing numerical simulation techniques. Moreover, it is imperative to conduct further research to investigate the extent of energy consumption, stability, and economic advantages associated with this particular form of connection. Further investigation is required to thoroughly examine the bond-slip constitutive relationship between steel and recycled steel fibre-reinforced concrete.

Acknowledgement: The authors thank Yunnan International Joint R&D Center of Smart Agriculture and Water Security, Yunnan Agricultural University, Kunming, 650201, China for their materials, laboratory service, and research funding support.

Funding Statement: This research was supported by the Key R&D Projects in Yunnan Province under Grant Number 202203AC100004. Additional funding was provided by the Major Science and Technology Project of the Ministry of Water Resources under Grant Number SKS-2022057. The authors acknowledge the financial support received from the Key R&D Projects in Yunnan Province and the Major Science and Technology Project of the Ministry of Water Resources for conducting this study.

Author Contributions: The authors confirm contribution to the paper as follows: study conception and design: J. L., I. S.; data collection: I. S. and Y. P.; analysis and interpretation of results: Y. P., I. S., A. R. and M. M. R.; draft manuscript preparation: I. S., H. R. A. and J. L. All authors reviewed the results and approved the final version of the manuscript.

Availability of Data and Materials: Not applicable.

Conflicts of Interest: The authors declare that they have no conflicts of interest to report regarding the present study.

References

1. Gao, D., Zhu, W., Fang, D., Tang, J., Zhu, H. (2022). Shear behavior analysis and capacity prediction for the steel fiber reinforced concrete beam with recycled fine aggregate and recycled coarse aggregate. *Structures, 37,* 44–55.
2. Yang, H., Huang, Y., Lv, L. (2022). Bond behavior between recycled aggregate concrete and steel rebar subjected to biaxial lateral pressure. *Structures, 41,* 139–146.
3. Yang, C., Shah, I., Jing, W., Khan, N., Jing, L. (2022). Comprehensive test and evaluation analysis of permeable concrete (PC) clogging by using steel slag. *Advances in Civil Engineering, 2022,* 2866776.
4. Shah, I., Li, J., Yang, S., Zhang, Y., Anwar, A. (2022). Experimental investigation on the mechanical properties of natural fiber reinforced concrete. *Journal of Renewable Materials, 10(5),* 1307–1320.
5. Shah, I., Jing, L., Fei, Z. M., Yuan, Y. S., Farooq, M. U. et al. (2021). A review on chemical modification by using sodium hydroxide (NaOH) to investigate the mechanical properties of sisal, coir and hemp fiber reinforced concrete composites. *Journal of Natural Fibers, 19(13),* 5133–5151.
6. Nižetić, S., Djilali, N., Papadopoulos, A., Rodrigues, J. J. (2019). Smart technologies for promotion of energy efficiency, utilization of sustainable resources and waste management. *Journal of Cleaner Production, 231,* 565–591.
7. Qin, X., Kaewunruen, S. (2022). Environment-friendly recycled steel fibre reinforced concrete. *Construction and Building Materials, 327,* 126967.
8. Katzer, J., Skoratko, A. (2022). Using 3D printed formworks for the creation of steel fibre reinforced concrete-plastic columns. *Construction and Building Materials, 337,* 127586.

9. Xie, J., Li, J., Lu, Z., Li, Z., Fang, C. et al. (2019). Combination effects of rubber and silica fume on the fracture behaviour of steel-fibre recycled aggregate concrete. *Construction and Building Materials, 203,* 164–173.
10. Makul, N., Fediuk, R., Amran, M., Zeyad, A. M., Klyuev, S. et al. (2021). Design strategy for recycled aggregate concrete: A review of status and future perspectives. *Crystals, 11(6),* 695.
11. Majhi, R. K., Nayak, A. N. (2020). Production of sustainable concrete utilising high-volume blast furnace slag and recycled aggregate with lime activator. *Journal of cleaner production, 255,* 120188.
12. Alhawat, M., Ashour, A. (2019). Bond strength between corroded steel reinforcement and recycled aggregate concrete. *Structures, 19,* 369–385.
13. Liu, S., Bai, C., Zhang, J., Zhao, J., Hu, Q. (2022). Experimental and theoretical study on bonding performance of FRP bars-Recycled aggregate concrete. *Construction and Building Materials, 361,* 129614.
14. Kim, J. (2022). Influence of quality of recycled aggregates on the mechanical properties of recycled aggregate concretes: An overview. *Construction and Building Materials, 328,* 127071.
15. Prince, M., Singh, B. (2015). Bond strength of deformed steel bars in high-strength recycled aggregate concrete. *Materials and Structures, 48(12),* 3913–3928.
16. Zhao, Y., Lin, H., Wu, K., Jin, W. (2013). Bond behaviour of normal/recycled concrete and corroded steel bars. *Construction and Building Materials, 48,* 348–359.
17. Seara-Paz, S., González-Fonteboa, B., Eiras-López, J., Herrador, M. F. (2014). Bond behavior between steel reinforcement and recycled concrete. *Materials and structures, 47(1),* 323–334.
18. Hameed, R., Akmal, U., Khan, Q. S., Cheema, M. A., Riaz, M. R. (2020). Effect of fibers on the bond behavior of deformed steel bar embedded in recycled aggregate concrete. *Mehran University Research Journal of Engineering & Technology, 39(4),* 846–858.
19. He, Z. J., Chen, Y., Ma, Y. N., Zhang, X. J., Jin, Y. X. et al. (2021). The study on bond-slip constitutive model of steel-fiber high-strength recycled concrete. *Structures, 34,* 2134–2150.
20. Rafi, M. (2019). Study of bond properties of steel rebars with recycled aggregate concrete. Analytical modeling. *Strength of Materials, 51,* 166–174.
21. Fang, H., Lin, B., Liang, W., Yao, Y. (2023). Constitutive model of interfacial bond-slip between steel fibers and concrete matrix after exposing to high temperature. *Journal of Building Engineering, 77,* 107569.
22. Kim, S. W., Yun, H. D., Park, W. S., Jang, Y. I. (2015). Bond strength prediction for deformed steel rebar embedded in recycled coarse aggregate concrete. *Materials & Design, 83,* 257–269.
23. Hamad, B. S., Abou Haidar, E. Y. (2011). Effect of steel fibers on bond strength of hooked bars in high-strength concrete. *Journal of Materials in Civil Engineering, 23(5),* 673–681.
24. Hameed, R., Turatsinze, A., Duprat, F., Sellier, A. (2013). Bond stress-slip behaviour of steel reinforcing bar embedded in hybrid fiber-reinforced concrete. *KSCE Journal of Civil Engineering, 17,* 1700–1707.
25. Rao, A., Jha, K. N., Misra, S. (2007). Use of aggregates from recycled construction and demolition waste in concrete. *Resources, Conservation and Recycling, 50(1),* 71–81.
26. Behera, M., Bhattacharyya, S., Minocha, A., Deoliya, R., Maiti, S. (2014). Recycled aggregate from C&D waste & its use in concrete–A breakthrough towards sustainability in construction sector: A review. *Construction and building materials, 68,* 501–516.
27. Xiao, J., Falkner, H. (2007). Bond behaviour between recycled aggregate concrete and steel rebars. *Construction and Building Materials, 21(2),* 395–401.
28. Kim, S. W., Yun, H. D. (2013). Influence of recycled coarse aggregates on the bond behavior of deformed bars in concrete. *Engineering Structures, 48,* 133–143.
29. Zhou, L. A., Chen, J. L. (2011). Study on compressive strength of recycled aggregate brick with construction waste. *Key Engineering Materials, 477,* 301–307.
30. Zhang, Y., Deng, M., Li, T., Dong, Z. (2021). Strengthening of flexure-dominate RC columns with ECC jackets: Experiment and analysis. *Engineering Structures, 231,* 111809.

31. Wu, K., Zheng, H., Shi, N., Chen, F., Xu, J. (2020). Analysis of the bond behavior difference in steel and steel fiber reinforced concrete (SSFRC) composite member with circular section. *Construction and Building Materials, 264,* 120142.
32. Chalioris, C. E., Kosmidou, P. M. K., Karayannis, C. G. (2019). Cyclic response of steel fiber reinforced concrete slender beams: An experimental study. *Materials, 12(9),* 1398.